Provided for non-commercial research and education use.
Not for reproduction, distribution or commercial use.

This article appeared in a journal published by Elsevier. The attached copy is furnished to the author for internal non-commercial research and education use, including for instruction at the authors institution and sharing with colleagues.

Other uses, including reproduction and distribution, or selling or licensing copies, or posting to personal, institutional or third party websites are prohibited.

In most cases authors are permitted to post their version of the article (e.g. in Word or Tex form) to their personal website or institutional repository. Authors requiring further information regarding Elsevier's archiving and manuscript policies are encouraged to visit:

http://www.elsevier.com/copyright

Author's personal copy

Journal of Biomechanics 44 (2011) 1253–1258

Contents lists available at ScienceDirect

Journal of Biomechanics

journal homepage: www.elsevier.com/locate/jbiomech
www.JBiomech.com

Leg stiffness increases with speed to modulate gait frequency and propulsion energy

Seyoung Kim, Sukyung Park*

Department of Mechanical Engineering, Korea Advanced Institute of Science and Technology (KAIST), 335 Gwahangno, Yuseong-gu, Daejeon 305-701, Republic of Korea

ARTICLE INFO

Article history:
Accepted 17 February 2011

Keywords:
Leg stiffness
Compliant walking model
Elastic energy
Human walking
Gait speed

ABSTRACT

Bipedal walking models with compliant legs have been employed to represent the ground reaction forces (GRFs) observed in human subjects. Quantification of the leg stiffness at varying gait speeds, therefore, would improve our understanding of the contributions of spring-like leg behavior to gait dynamics. In this study, we tuned a model of bipedal walking with damped compliant legs to match human GRFs at different gait speeds. Eight subjects walked at four different gait speeds, ranging from their self-selected speed to their maximum speed, in a random order. To examine the correlation between leg stiffness and the oscillatory behavior of the center of mass (CoM) during the single support phase, the damped natural frequency of the single compliant leg was compared with the duration of the single support phase. We observed that leg stiffness increased with speed and that the damping ratio was low and increased slightly with speed. The duration of the single support phase correlated well with the oscillation period of the damped complaint walking model, suggesting that CoM oscillations during single support may take advantage of resonance characteristics of the spring-like leg. The theoretical leg stiffness that maximizes the elastic energy stored in the compliant leg at the end of the single support phase is approximated by the empirical leg stiffness used to match model GRFs to human GRFs. This result implies that the CoM momentum change during the double support phase requires maximum forward propulsion and that an increase in leg stiffness with speed would beneficially increase the propulsion energy. Our results suggest that humans emulate, and may benefit from, spring-like leg mechanics.

© 2011 Elsevier Ltd. All rights reserved.

1. Introduction

Bipedal walking models with compliant legs have been employed to describe gait dynamics that are a function of the compliant properties of the leg, such as 'M-shaped' vertical ground reaction forces (GRFs) (Blickhan, 1989; Geyer et al., 2005, 2006; Whittington and Thelen, 2009). As a system parameter, the stiffness of a compliant walking model determines the system characteristics, such as the gait cycle period and the amplitude ratio of center of mass (CoM) oscillations to an external force. For example, the stiffness and the total system energy differentiate the domains of walking and running (Geyer et al., 2006). Therefore, quantification of the leg stiffness of a compliant walking model and the change in stiffness at different gait speeds would allow a better understanding of the contributions of spring-like leg behavior to gait dynamics. Previous studies have reported leg compliance as a form of vertical lower limb stiffness (Farley and Gonzalez, 1996; Holt et al., 2000; Holt et al., 2003; Rebula et al., 2009), which was defined as the ratio of the GRF to the CoM displacement. However, leg stiffness determines system dynamics; therefore, determining the lower limb stiffness using full dynamic equations would more directly quantify the contribution of leg stiffness to gait dynamics. In addition, using this method to determine the lower limb stiffness allows changes in leg stiffness to be interpreted from a system dynamics perspective.

In this study, we calculated the effective leg stiffness of human subjects walking at four different speeds by simulating a damped compliant walking model that was slightly modified from existing compliant walking models (Geyer et al., 2006; Whittington and Thelen, 2009). The stiffness and damping ratios were determined using model simulations that best matched human GRF data. To examine correlations between leg stiffness and the oscillatory behavior of the CoM during the single support phase, the damped natural frequency of the single compliant leg was compared with the duration of the single support phase. To interpret the change in leg stiffness with gait speed from an energetic perspective, the theoretical leg stiffness that maximized the elastic energy stored in the compliant leg at the end of the single support phase was calculated as a function of leg stiffness and gait speed and was then compared with human leg stiffness data.

* Corresponding author. Tel.: +82 42 350 3230; fax: +82 42 350 5230.
E-mail address: sukyungp@kaist.ac.kr (S. Park).

0021-9290/$ - see front matter © 2011 Elsevier Ltd. All rights reserved.
doi:10.1016/j.jbiomech.2011.02.072

Author's personal copy

2. Methods

2.1. Subjects

Eight healthy young subjects (7M/1F, 23 ± 2 years) volunteered for this study. In a questionnaire, they reported no history of leg injuries or balance disorders. After a detailed explanation of the purpose of the research and prior to testing, all subjects signed an informed consent form approved by the Institutional Review Board of the Korea Advanced Institute of Science and Technology (KAIST). The average height and weight of the subjects were 1.68 ± 0.06 m and 66.7 ± 10.9 kg, respectively.

2.2. Protocols

The subjects walked on a straight 12-m-long, 1-m-wide walkway at four different speeds, including their self-selected natural speed and their maximum speed. We set the gait frequency intervals to one-third of the difference between the frequencies corresponding to the natural and maximum walking speeds. A metronome (Dual Metronome Reference Pitch Generator SMT-1000, SAMICK®) with a steady beat, which guided steady-state walking, generated three sets of four randomly ordered gait frequency cues to each subject. The details of the experimental procedure have been presented previously (Yeom and Park, 2010).

2.3. Measurement

For each trial, body kinematics and kinetics were sampled at 200 Hz using motion capture cameras (Motion Analysis, Hawk®) and three force plates (AMTI, AccuGait®), respectively. Three optical markers, located at the sacrum and on both ankles, were used. The sacral marker was used as an initial position to calculate the trajectory of the CoM. The ankle markers were used to determine leg configurations. Optical marker positions and GRFs were 5th-order Butterworth low-pass filtered with cutoff frequencies of 10 Hz for the motion capture data and 30 Hz for the force plate data. The velocity and the trajectory of the CoM were calculated by integrating the accelerations obtained from the GRF data (Donelan et al., 2002a; Yeom and Park, 2010).

2.4. Compliant walking model

To calculate leg stiffness as a function of walking speed, the human body was modeled as a lumped mass on top of two massless, compliant legs connected to a curved foot (Fig. 1). We added a damper to an existing compliant walking model (Geyer et al., 2006; Whittington and Thelen, 2009). The compliant leg was defined as a radial telescoping leg that deflects in the linear direction but can transmit forces in tangential directions (Whittington and Thelen, 2009). A passive spring provided a compliant mechanism to absorb collision impacts and to generate push-off impulses, whereas the damper restrained excessive motion of the CoM. Both the spring and damper were assumed to be time-invariant linear components at a given walking speed. A curved foot was used to emulate center of pressure (CoP) excursions (Adamczyk et al., 2006; Whittington and Thelen, 2009).

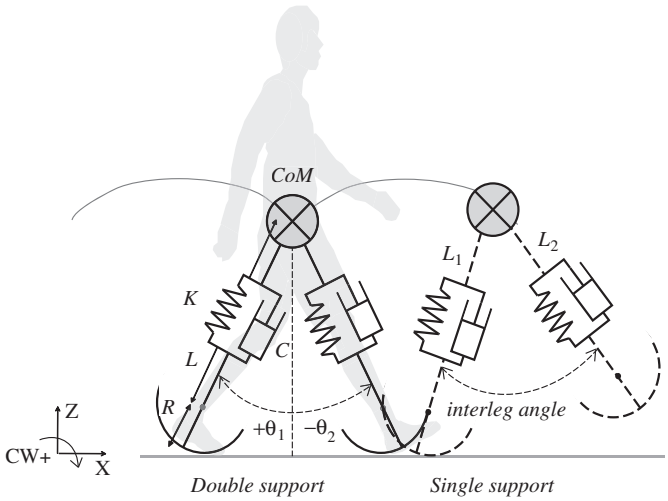

Fig. 1. Schematic of the biomechanical walking model. Human body was modeled with two massless, compliant legs with curved feet. The parameters K, C, θ, L and R indicate the spring constant, damping constant, leg angle with respect to the vertical axis, compliant leg length and radius of the curved foot, respectively. The subscripts '1' and '2' indicate the trailing leg and the leading leg, respectively.

The equations of motion for the compliant walking model were derived using a *Newton–Euler* formulation under the assumption that the legs were telescoping. The derived equations were compared with those from a *Lagrangian* formulation. The dynamic equation of the model under gravity (g) can be written as follows (Whittington and Thelen, 2009):

$$\begin{bmatrix} MR\sin\theta_1 & M \\ ML_1^2+2MRL_1\cos\theta_1+MR^2 & MR\sin\theta_1 \end{bmatrix}\begin{bmatrix} \ddot{\theta}_1 \\ \ddot{L}_1 \end{bmatrix} =$$

$$\begin{bmatrix} -MR\dot{\theta}_1^2\cos\theta_1+ML_1\dot{\theta}_1^2+MR\dot{\theta}_1^2\cos\theta_1-Mg\cos\theta_1+KL_0-KL_1 \\ +(KL_0-KL_2)\left(\frac{L_2\cos(\theta_1-\theta_2)+R\cos\theta_1}{L_2+R\cos\theta_2}\right)-C\dot{L}_1-C\dot{L}_2\left(\frac{L_2\cos(\theta_1-\theta_2)+R\cos\theta_1}{L_2+R\cos\theta_2}\right) \\ -2ML_1\dot{L}_1\dot{\theta}_1-3MR\dot{L}_1\dot{\theta}_1\cos\theta_1+MRL_1\dot{\theta}_1^2\sin\theta_1+MR\dot{L}_1\dot{\theta}_1\cos\theta_1+MgL_1\sin\theta_1 \\ +(KL_0-KL_2)\left(\frac{RL_2\sin\theta_2-L_1L_2\sin(\theta_1-\theta_2)-RL_1\sin\theta_1}{L_2+R\cos\theta_2}\right)-C_2\dot{L}_2\left(\frac{RL_2\sin\theta_2-L_1L_2\sin(\theta_1-\theta_2)-RL_1\sin\theta_1}{L_2+R\cos\theta_2}\right) \end{bmatrix}$$

where M, R, θ, $\dot{\theta}$, L, $\dot{L}$, L_0, K and C are the body mass, curved foot radius, leg angle, leg angular velocity, leg length, leg length velocity, slack length, spring constant and damping constant, respectively. The subscripts '1' and '2' indicate the trailing leg and the leading leg, respectively.

The double support phase begins when the leading leg hits the ground and continues until the trailing leg spring reaches its slack length, where the single support phase begins. Then, the trailing leg is repositioned ahead of the body's CoM at a given interleg angle and becomes the leading leg for the next step. When the leading leg hits the ground, i.e., touchdown, the single support phase is finished. The CoM motion is constrained by one (single support phase) or two (double support phase) compliant legs, depending on the gait phase.

We obtained spring and damping constants from an optimization that minimized the least square error between the GRF data and the model simulation over one-step cycle, which consists of double and single support phases. The optimization was performed by sequential quadratic programming using a non-linear equation solver (fmincon, Matlab®). To determine whether the optimization found a global solution, we repeated the optimization multiple times over a wide range of random initial conditions. Other model parameters, such as the initial state and the interleg angle, were determined from empirical data. The curved foot radius was set to 0.3 m based on previous literature (Adamczyk et al., 2006; Whittington and Thelen, 2009).

We tested whether the leg stiffness and the damping ratio changed as a function of walking speed. To determine whether the system compliance contributes to the oscillatory behavior of the CoM, we compared the damped natural frequency (ω_d) of the single compliant leg, which is defined as $\omega_d=\omega_n\sqrt{1-\zeta^2}$, $\omega_n=\sqrt{K/M}$, where M, K and ζ are the body mass, leg stiffness and damping ratio, respectively, with the duration of the single support phase. During the single support phase, the CoM freely bounces forward atop the single stance leg, whereas the motion of the CoM is under closed-loop kinematic constraint by two legs during the double support phase. Therefore, the effect of the stiffness on the system oscillation could be better demonstrated during the single support phase as opposed to the whole support phase for one foot, which includes both single and double support phase. We also calculated the elastic potential energy stored in the compliant leg ($(1/2)K\Delta L^2$, where ΔL is leg length change) at the end of the single support phase, which serves as propulsion energy during push-off, to interpret the change in leg stiffness with gait speed from an energetic perspective. The elastic energy was calculated as a function of both leg stiffness (14–28 kN/m) and gait speed (0.8–2.2 m/s). Initial states, interleg angles, and damping ratios were regressed as a function of walking speed (Fig. 2). The average body weight and height of all subjects were used for the parameter study. The significance of all of the reported trends from the parameter study was tested using regression analysis with a significance level of $p<0.05$.

3. Results

Model simulations reproduced the trajectories of the GRFs with a goodness of fit ($R^2=0.81\pm0.06$) for all subjects. A slightly better match was achieved for trials at the self-selected and intermediate gait speeds than for trials at the maximum gait speed (Fig. 3). The leg stiffness and the damping ratio significantly increased as a function of gait speed ($p<0.05$). The averaged slopes of the dimensionless stiffness (normalized by body weight divided by height) and the damping ratio with respect to a unit speed change were 39.82 ± 12.71 and 0.036 ± 0.013 s/m,

Author's personal copy

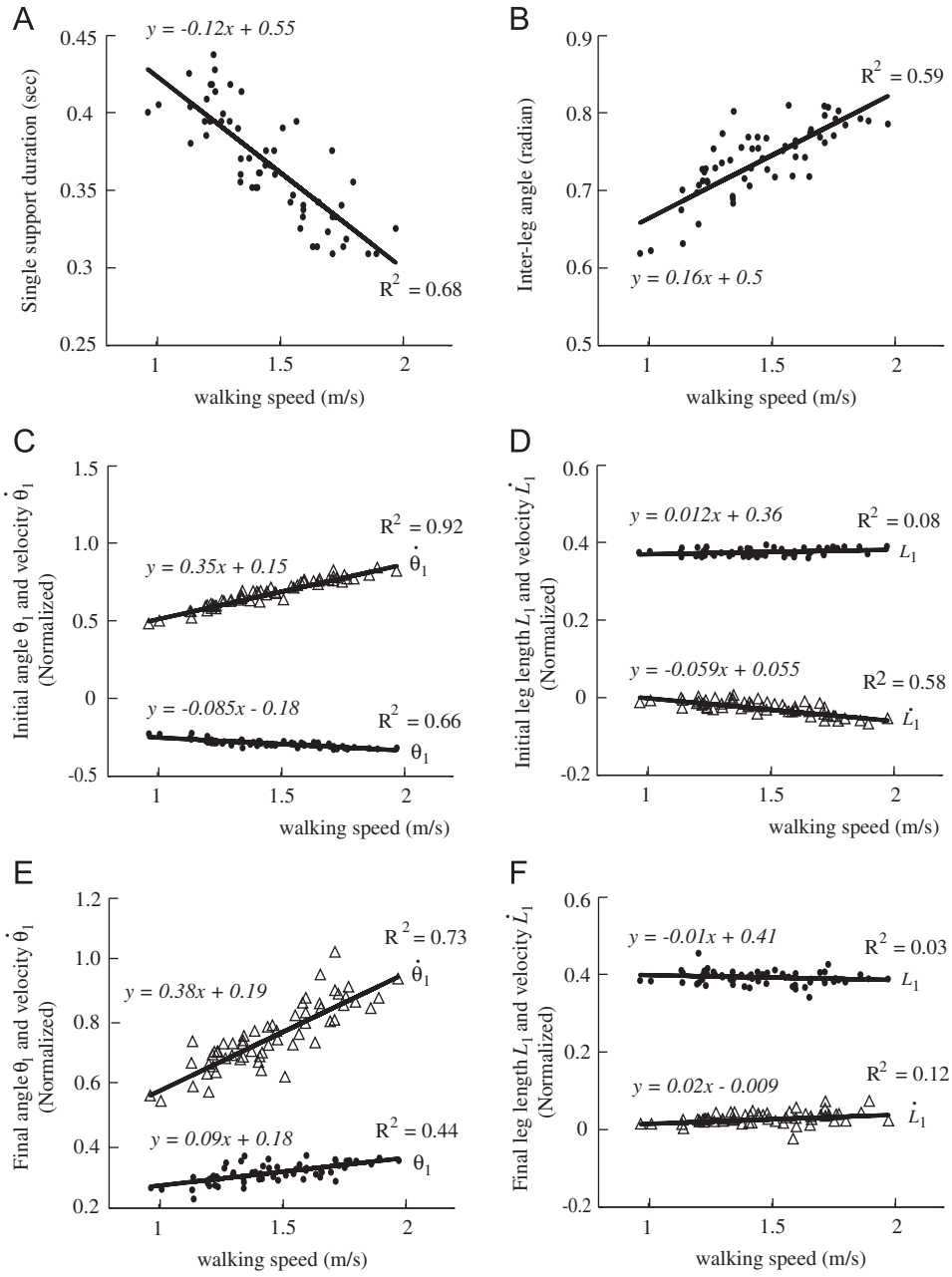

Fig. 2. Empirical data for the gait parameters. (A) Duration of the single support phase, (B) interleg angles, (C) initial angles and the angular velocities for the single support phase, (D) initial spring leg lengths and the velocities for the single support phase, (E) final angles and the angular velocities for the single support phase and (F) final spring leg lengths and the velocities for the single support phase at the corresponding walking speeds. The values were estimated from the model using the empirical data separately for each subject. The solid lines indicate the linear regression slopes of the empirical data for all subjects as a function of gait speed. The full equations for the curve fits are displayed in the form of $y=ax+b$.

respectively (Fig. 4). Damping ratios ranged from 0.03 to 0.08 and were necessary to robustly generate repeated steps that reproduced the human data with various initial conditions.

The duration of the single support phase correlated well with the period of the damped natural frequency of the single compliant leg (slope=1.1, R^2=0.82; Fig. 5). The model simulation of the elastic energy stored in the complaint leg at the end of the swing phase was plotted as a function of the spring constant and the gait speed (Fig. 6). The leg stiffness trajectory that maximized the elastic potential energy was well approximated by the experimental leg stiffness used to match the model GRFs to the human GRFs.

4. Discussion

A damped compliant walking model was able to reproduce a one-step gait cycle that consisted of double and single support phases. The effective leg stiffness determined using the full dynamics of the bipedal walking model in this study ranged between the vertical limb stiffness (defined by the ratio of the force change to the displacement change) during the double (K_{ds}) and single support phases (K_{ss}), as reported previously (Rebula et al., 2009). The duration of the single support phase correlated well with the oscillation period of the damped complaint walking model, suggesting that CoM oscillations during the single support

Author's personal copy

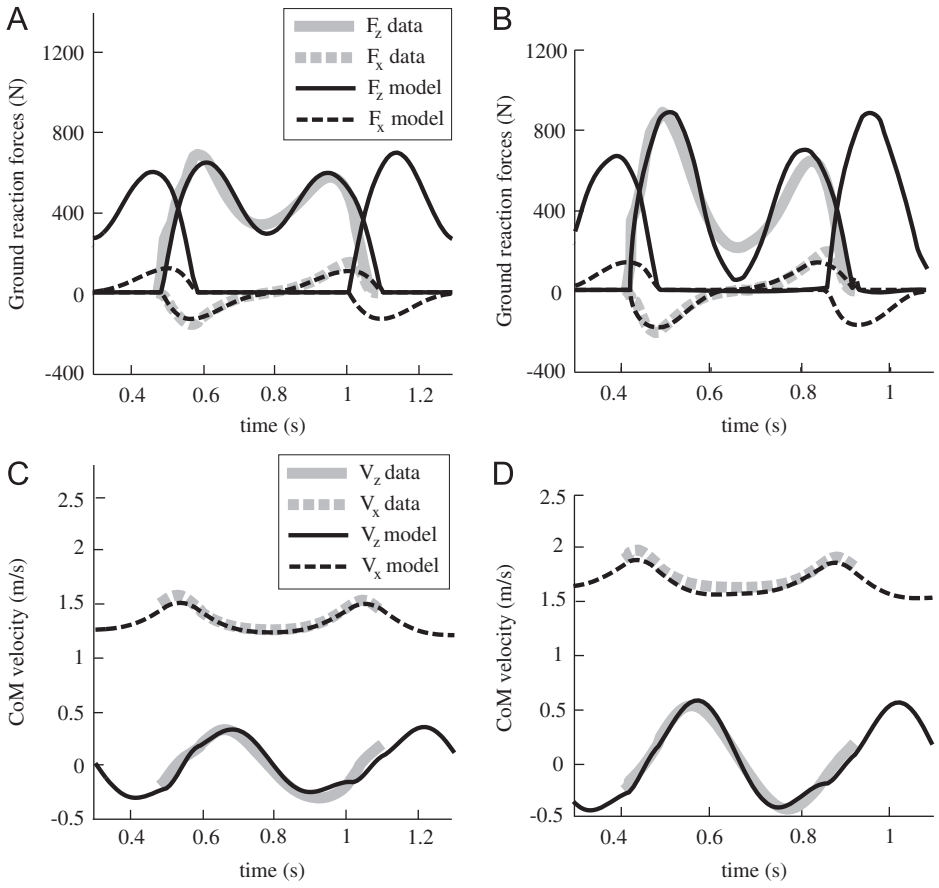

Fig. 3. GRFs and CoM velocities (gray lines) and the model simulations (black lines). The solid lines and the dotted lines represent the vertical and horizontal directions, respectively. The GRFs and the CoM velocities at the preferred and maximum walking speeds are shown in the left (A, C) and right (B, D) columns, respectively.

phase may take advantage of resonance characteristics of the spring-like leg. The theoretical leg stiffness that maximized the elastic energy stored in the compliant leg at the end of the single support phase was approximated by the empirical leg stiffness. This result implies that the CoM momentum change during the double support requires maximum forward propulsion and that an increase in leg stiffness with speed would beneficially increase the propulsion energy.

The reasonable match of the model simulation to the data implies that humans emulate spring-like leg mechanics and modulate the apparent leg stiffness. However, without any further physiological modeling or experimentation, our results do not necessarily indicate that the actual muscle behaves as a single spring. For example, the mechanical spring component could store elastic potential energy when the leg is compressed and release the energy during leg extension as a form of kinetic energy for forward propulsion. Therefore, unless the energy is dissipated by damping or friction, the compliant walking model does not require an energy input mechanism to maintain steady walking. In human walking, however, oscillatory CoM movement is achieved by lower limb joint kinematics and requires active positive and negative muscle work (Donelan et al., 2002b, a). Therefore, the results of the mechanical energy analysis using the compliant leg model should not be interpreted as corresponding metabolic energy expenditure. Moreover, multi-joint stiffness characteristics were lumped into whole-leg stiffness. Thus, the current model does not specify how changes in leg stiffness might be attributed to changes at each joint. Hypothetically, whole-leg stiffness could be assumed to be a combination of knee, ankle and metatarsal joint stiffnesses, with the coefficients being a function of leg geometry. The increase in joint stiffness could be achieved by increased muscle forces that reduce the range of joint motion (Davis and DeLuca, 1996; Holt et al., 2003; Zeni and Higginson, 2009). Therefore, the increase in whole-leg stiffness might be related to an increase in the knee and ankle joint muscle tension (Yang and Winter, 1985; Riley et al., 2001; Zeni et al., in press). The relative contribution of the stiffness of each joint to the change in the whole-leg stiffness, however, has not been consistently reported. Muscle tension in the knee joint was reported to change more dramatically with gait speed than muscle tension in the ankle joint (Yang and Winter, 1985; Teixeira-Salmela et al., 2008; Zeni et al., in press), suggesting that the knee joint plays a more important role in the change in the whole-leg stiffness than the ankle joint stiffness does. However, other leg muscle groups related to ankle and hip joint moment (e.g., soleus and gluteus maximus) have been reported to be more sensitive with gait speed than muscle groups (Liu et al., 2008; Neptune et al., 2008). To quantify the contribution of the stiffness of each joint to whole-leg stiffness, multi-joint dynamic analysis needs to be performed at different gait speeds. Similarly, push-off propulsion during the double support phase using elastic energy stored in the compliant leg must be distributed to ankle, knee and hip joint. Previous studies have reported that ankles provide most of the push-off in a normal gait (Yang and Winter, 1985; Lewis and Ferris, 2008; Liu et al., 2008; Neptune et al., 2008; Teixeira-Salmela et al., 2008; Simonsen et al., 2010), and the increased contribution of the knee joints was reported at faster gaits (Teixeira-Salmela et al., 2008; Zeni et al., in press). Therefore, the distribution of the push-off propulsion at each joint depends on the gait.

Although our model dissipates energy through a damping component, small damping ratios (<0.1) emulated the steady-state human GRF data reasonably well. To achieve limit cycle

Author's personal copy

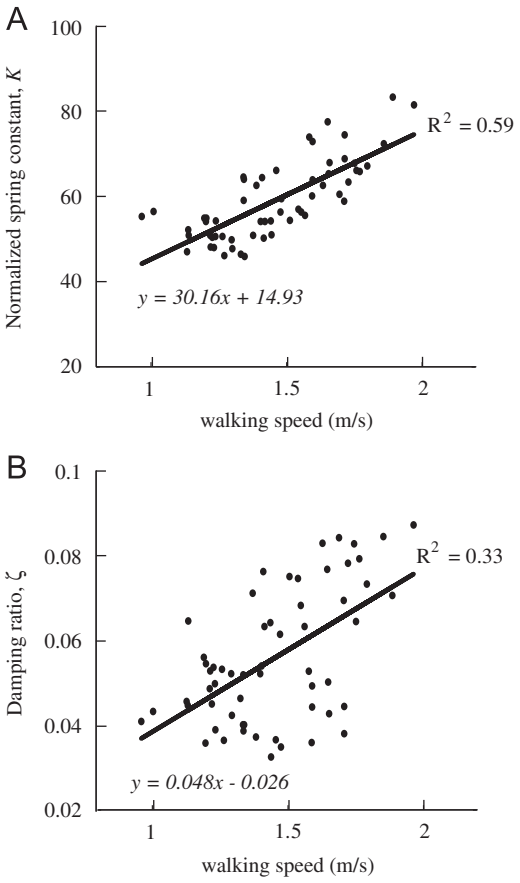

Fig. 4. Spring constant (A) and the damping ratio (B) as a function of gait speed obtained from the optimization that minimized the fitting error. The spring constants were normalized by the subjects' weights divided by their heights. The solid lines indicate the linear regression slopes. The full equations for the curve fits are displayed in the form of $y=ax+b$.

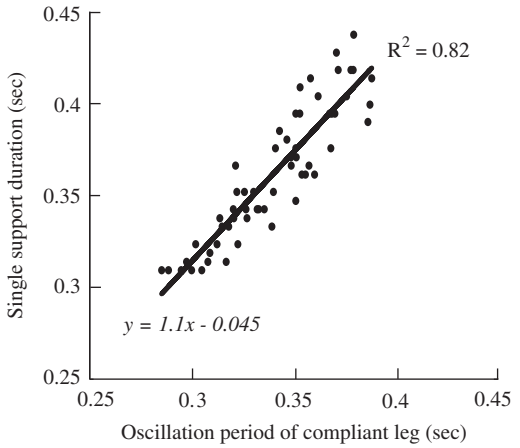

Fig. 5. Duration of the single support phase and the period of oscillation of the compliant walking model. The single support duration was closely related to the damped natural frequency of the compliant leg (linear regression slope=1.1, R^2=0.82). The full equation for the curve fit is displayed in the form of $y=ax+b$.

behavior, however, active energy input was required to compensate for energy loss. One possible candidate, among many ways to provide the additional energy, is to apply a control force or torque to the system in a feedback or feed-forward manner. Quantitative postural control models using feedback controllers have been

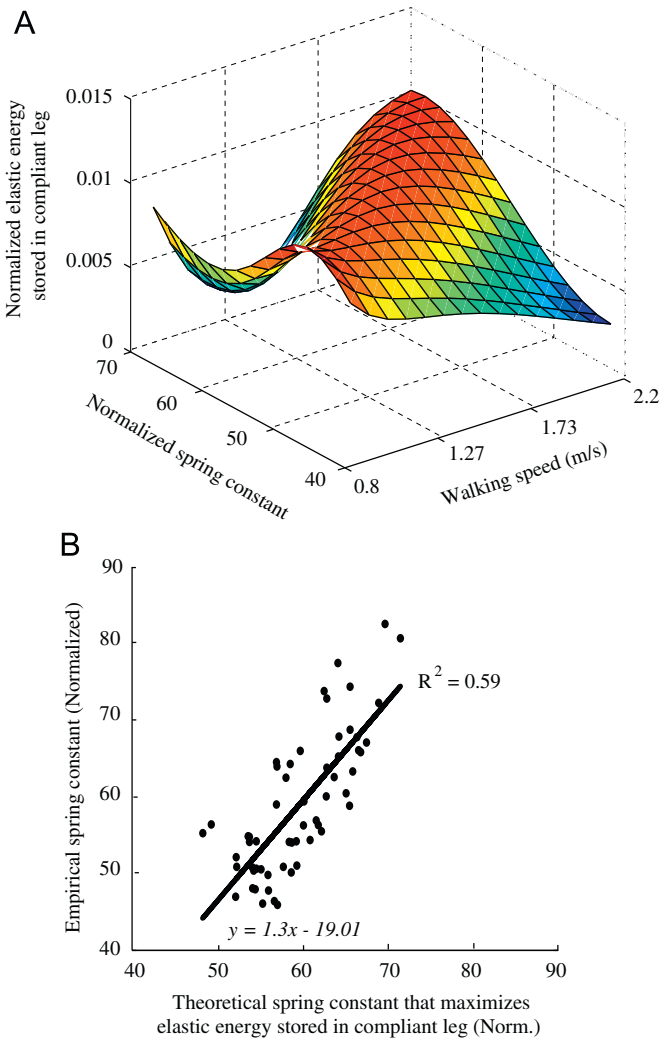

Fig. 6. (A) Model simulation of the elastic energy stored in the compliant leg as a function of the spring constant and the gait speed. (B) Theoretical spring constants that maximize the elastic energy stored in compliant leg and the leg stiffness calculated from the subject data at the corresponding walking speeds. (A) Elastic energy was calculated using the formula for the spring potential energy $(1/2)K\Delta L^2$ at the end of the single support phase. (B) Theoretical spring constant as a function of walking speed matched well with the experimental leg stiffness (linear regression slope=1.3, R^2=0.59). The full equation for the curve fit is displayed in the form of $y=ax+b$.

proposed to describe the central nervous system's (CNS) postural strategy changes (Van Der Kooij et al., 1999; Peterka, 2002; Park et al., 2004; Kuo, 2005; Welch and Ting, 2008; Kim et al., 2009). Similarly, a steady gait could also be achieved through CNS feedback control based on the state error between the desired and estimated current states. Due to the small damping that does not greatly dissipate the energy during the gait cycle, we expect that the feedback control input would be small and that the stiffness and its scaling trend would not change significantly for the feedback-controlled gait model relative to the current results. Regardless of the limited physiological perspective of our results discussed above, the current model provides a basic understanding of how spring-like leg behavior in human walking could contribute to gait dynamics and energetics. Therefore, the suggested model could be used to quantify changes in gait dynamics among different walking conditions and/or subject groups, such as for gait performance assessment for the elderly or for health care patients.

Author's personal copy

Conflict of interest statement

None declared.

Acknowledgments

This research was supported by the Basic Science Research Program through the National Research Foundation of Korea (NRF) funded by the Ministry of Education, Science and Technology (#2010-0013306) and by the Unmanned Technology Research Center (UTRC) at the Korea Advanced Institute of Science and Technology (KAIST), originally funded by DAPA, ADD. The authors thank Jin Yeom and Heewon Park for their contributions to data collection.

References

Adamczyk, P.G., Collins, S.H., Kuo, A.D., 2006. The advantages of a rolling foot in human walking. Journal of Experimental Biology 209, 3953–3963.

Blickhan, R., 1989. The spring-mass model for running and hopping. Journal of Biomechanics 22, 1217–1227.

Davis, R.B., DeLuca, P.A., 1996. Gait characterization via dynamic joint stiffness. Gait and Posture 4, 224–231.

Donelan, J.M., Kram, R., Kuo, A.D., 2002a. Simultaneous positive and negative external mechanical work in human walking. Journal of Biomechanics 35, 117–124.

Donelan, J.M., Kram, R., Kuo, A.D., 2002b. Mechanical work for step-to-step transitions is a major determinant of the metabolic cost of human walking. Journal of Experimental Biology 205, 3717–3727.

Farley, C.T., Gonzalez, O., 1996. Leg stiffness and stride frequency in human running. Journal of Biomechanics 29, 181–186.

Geyer, H., Seyfarth, A., Blickhan, R., 2005. Spring-mass running: simple approximate solution and application to gait stability. Journal of Theoretical Biology 232, 315–328.

Geyer, H., Seyfarth, A., Blickhan, R., 2006. Compliant leg behaviour explains basic dynamics of walking and running. Proceedings of the Royal Society B: Biological Sciences 273, 2861–2867.

Holt, K.G., Fonseca, S.T., Lafiandra, M.E., 2000. The dynamics of gait in children with spastic hemiplegic cerebral palsy: theoretical and clinical implications. Human Movement Science 19, 375–405.

Holt, K.G., Wagenaar, R.C., LaFiandra, M.E., Kubo, M., Obusek, J.P., 2003. Increased musculoskeletal stiffness during load carriage at increasing walking speeds maintains constant vertical excursion of the body center of mass. Journal of Biomechanics 36, 465–471.

Kim, S., Horak, F.B., Carlson-Kuhta, P., Park, S., 2009. Postural feedback scaling deficits in Parkinson's disease. Journal of Neurophysiology 102, 2910–2920.

Kuo, A.D., 2005. An optimal state estimation model of sensory integration in human postural balance. Journal of Neural Engineering 2, S235–S249.

Lewis, C.L., Ferris, D.P., 2008. Walking with increased ankle pushoff decreases hip muscle moments. Journal of Biomechanics 41, 2082–2089.

Liu, M.Q., Anderson, F.C., Schwartz, M.H., Delp, S.L., 2008. Muscle contributions to support and progression over a range of walking speeds. Journal of Biomechanics 41, 3243–3252.

Neptune, R.R., Sasaki, K., Kautz, S.A., 2008. The effect of walking speed on muscle function and mechanical energetics. Gait and Posture 28, 135–143.

Park, S., Horak, F.B., Kuo, A.D., 2004. Postural feedback responses scale with biomechanical constraints in human standing. Experimental Brain Research 154, 417–427.

Peterka, R.J., 2002. Sensorimotor integration in human postural control. Journal of Neurophysiology 88, 1097–1118.

Rebula, J.R., O'Connor, S.M., Kuo, A.D., 2009. Human walking and running: it's all in the redirection. Dynamic Walking, 2009.

Riley, P.O., Della Croce, U., Kerrigan, D.C., 2001. Effect of age on lower extremity joint moment contributions to gait speed. Gait and Posture 14, 264–270.

Simonsen, E.B., Moesby, L.M., Hansen, L.D., Comins, J., Alkjaer, T., 2010. Redistribution of joint moments during walking in patients with drop-foot. Clinical Biomechanics 25, 949–952.

Teixeira-Salmela, L.F., Nadeau, S., Milot, M.H., Gravel, D., Requiao, L.F., 2008. Effects of cadence on energy generation and absorption at lower extremity joints during gait. Clinical Biomechanics.

Van Der Kooij, H., Jacobs, R., Koopman, B., Grootenboer, H., 1999. A multisensory integration model of human stance control. Biological Cybernetics 80, 299–308.

Welch, T.D.J., Ting, L.H., 2008. A feedback model reproduces muscle activity during human postural responses to support-surface translations. Journal of Neurophysiology 99, 1032–1038.

Whittington, B.R., Thelen, D.G., 2009. A simple mass-spring model with roller feet can induce the ground reactions observed in human walking. Journal of Biomechanical Engineering, 131.

Yang, J.F., Winter, D.A., 1985. Surface EMG profiles during different walking cadences in humans. Electroencephalography and Clinical Neurophysiology 60, 485–491.

Yeom, J., Park, S., 2010. A gravitational impulse model predicts collision impulse and mechanical work during a step-to-step transition. Journal of Biomechanics 44, 59–67.

Zeni, J.A., Higginson, J.S., 2009. Dynamic knee joint stiffness in subjects with a progressive increase in severity of knee osteoarthritis. Clinical Biomechanics 24, 366–371.

Zeni, J.A., Higginson, J.S. Knee osteoarthritis affects the distribution of joint moments during gait. Knee, in press. doi:10.1016/j.knee.2010.04.003.